

# Purification and characterization of a novel acid-tolerant and heterodimeric $\beta$ -glucosidase from pumpkin (*Cucurbita moschata*) seed

Eui Young Kim,<sup>1,†</sup> Chang Woo Kwon,<sup>2,†</sup> and Pahn-Shick Chang<sup>1,2,3,4,\*</sup>

Department of Agricultural Biotechnology, Seoul National University, Seoul 08826, Republic of Korea,<sup>1</sup> Research Institute of Agriculture and Life Sciences, Seoul National University, Seoul 08826, Republic of Korea,<sup>2</sup> Center for Food and Bioconvergence, Seoul National University, Seoul 08826, Republic of Korea,<sup>3</sup> and Center for Agricultural Microorganism and Enzyme, Seoul National University, Seoul 08826, Republic of Korea<sup>4</sup>

Received 19 January 2021; accepted 16 April 2021  
Available online 30 May 2021

**A novel  $\beta$ -glucosidase was purified from pumpkin (*Cucurbita moschata*) seed by anion exchange chromatography and gel permeation chromatography, and its molecular mass was determined to be 42.8 kDa by gel permeation chromatography. The heterodimeric structure consisting of two subunits, free from disulfide bonds, was determined by native-PAGE analysis followed by zymography. The enzyme was maximally active at pH 4.0 and 70°C, and  $V_{max}$ ,  $K_m$ , and  $k_{cat}$  values were 0.078 units  $mg^{-1}$  protein, 2.22 mM, and 13.29  $min^{-1}$ , respectively, employing *p*-nitrophenyl- $\beta$ -D-glucopyranoside as the substrate. The high content of glycine determined by amino acid analysis implies that the enzyme possesses flexible conformations and interacts with cell membranes and walls in nature. Circular dichroism studies revealed that the high stability of the enzyme within the pH range of 2.0–10.0 is due to its reversible pH-responsive characteristics for  $\alpha$ -helix–antiparallel  $\beta$ -sheet interconversion.**

© 2021, The Society for Biotechnology, Japan. All rights reserved.

[**Key words:**  $\beta$ -Glucosidase; Pumpkin (*Cucurbita moschata*); Acid-tolerant properties; Secondary structure; Enzyme kinetics]

Isoflavones, a subclass of phytoestrogens, are natural plant compounds referred to as estrogen-like molecules due to their structural similarity to estradiol (17- $\beta$ -estradiol, E2), which allows binding to estrogen receptors. In addition to their estrogenic effects on the symptoms of postmenopausal syndrome, isoflavones exhibit antiangiogenic, anticancer, antioxidant, anti-inflammatory, antimicrobial, antiosteoporotic, proapoptotic, and antiproliferative activities (1–5). Three types of isoflavones, genistin, daidzin, and glycitin, are abundant in soybean. They exist predominantly as  $\beta$ -glycoside forms possessing sugar molecules, which make the compounds more soluble in water such that they can be stored easily in inactive and less toxic forms. However, chemical modifications such as glycosylation of genistin, daidzin, and glycitin make the compounds difficult to absorb in the small intestine when consumed as a raw food. Hence, they need to be hydrolyzed to the respective aglycones, e.g., genistein, daidzein, and glycitein, which enhance their bioavailability (6).

$\beta$ -Glucosidase ( $\beta$ -D-glucoside glucohydrolase, EC 3.2.1.21) catalyzes the hydrolysis of  $\beta$ -glucosidic linkages in amino-, aryl-, or alkyl- $\beta$ -D-glucosides, di- or oligosaccharides, and cyanogenic glucosides, which results in liberation of a free glucose unit and the corresponding aglycone. This enzyme has been found in all living organisms from prokaryotes to eukaryotes.  $\beta$ -Glucosidase plays diverse key roles in physiological processes, e.g., utilization of oligosaccharide substrates by bacteria and fungi; cell wall, pigment,

and cyanoglucoside metabolism in plants; and glucoside ceramide catabolism in human tissues (7). In addition, it has potential commercial applications in the food industry, e.g., liberation of aroma from wine grapes, transformation of isoflavones during soy-based food preparation, and hydrolysis of bitter compounds during the extraction of juices (8–10). Hence, the need to discover unique  $\beta$ -glucosidases from novel sources has been important for applications to various industries. In particular, generally recognized as safe plants are good resources because they can be applied to the product directly as a food additive without quantitative restrictions.

Pumpkin (*Cucurbita moschata*) seeds, also known as pepitas (Spanish) in North America, are edible, flat, oval-shaped green seeds that are often consumed as a salad topping, a stand-alone snack, or as an added crunchy ingredient in cookies. They have medicinal benefits, such as preventing breast, colon, and prostate cancers and reducing cholesterol, diabetes, and high blood pressure, and nutritional benefits, such as providing a great source of zinc, magnesium, and tryptophan (11–13). In addition, many researchers have recently used the combination of pumpkin seeds and soybean to produce nutritious tempeh and tofu and to reduce urinary incontinence (14–16). Therefore, determination of the  $\beta$ -glucosidase activity of pumpkin seeds will become necessary as the use of pumpkin seeds in combination with soy isoflavones increases.

In this study, we purified a novel heterodimeric  $\beta$ -glucosidase consisting of  $\alpha$ - and  $\beta$ -subunits from pumpkin seeds and

\* Corresponding author at: Department of Agricultural Biotechnology, Seoul National University, Seoul 08826, Republic of Korea. Fax: +82 2 873 5095.  
E-mail address: pschang@snu.ac.kr (P.-S. Chang).

† The first two authors contributed equally to this work.

characterized its catalytic and structural properties, which are important for understanding the role of  $\beta$ -glucosidase in combination with isoflavone.

## MATERIALS AND METHODS

**Materials** Pumpkin (*C. moschata*) seeds were purchased from a local farm in the Republic of Korea. The seeds were stored at 4°C until analysis. *p*-Nitrophenyl- $\beta$ -D-glucopyranoside (pNPG,  $\geq 98\%$ ), Trizma base ( $\geq 99.9\%$ ), *N,N,N',N'*-tetramethylethylenediamine, acetic acid ( $\geq 99\%$ ), 2-mercaptoethanol ( $\geq 99\%$ ), sodium dodecyl sulfate (SDS), glycerol ( $\geq 99\%$ ), and glycine ( $\geq 99\%$ ) were purchased from Sigma-Aldrich Co. (St. Louis, MO, USA). Ammonium sulfate (99.5%), citric acid (99.5%), sodium carbonate (anhydrous), sodium chloride (99.5%), and Triton X-100 were purchased from Junsei Chemical Co., Ltd. (Tokyo, Japan). Ammonium persulfate, a Bio-Rad protein assay kit, *N,N'*-methylenebis-acrylamide 37.5:1 solution, and bromophenol blue were purchased from Bio-Rad Laboratories, Inc. (Hercules, CA, USA). 4-Methylumbelliferyl- $\beta$ -D-glucoside (4-MUG) was purchased from Anaspec, Inc. (Fremont, CA, USA).

**Preparation of crude enzyme** Fresh pumpkin seeds (200 g) were ground using a blender and stored in 1.2 L of 20 mM Tris-HCl (pH 7.0) at 4°C. After centrifuging the mixture at 14,000  $\times$ g for 1 h, the supernatant was filtered using a 3  $\mu$ m membrane filter (Advantec MFS, Inc., Tokyo, Japan). Ammonium sulfate was added to the filtrate to obtain a 10% saturated solution, and then the solution was stirred overnight at 4°C using a magnetic stirrer and centrifuged at 14,000  $\times$ g for 1 h at 4°C. The precipitate was discarded, and the supernatant was brought to 80% ammonium sulfate saturation. After centrifuging the mixture at 14,000  $\times$ g for 1 h at 4°C, the precipitate was dialyzed against 20 mM Tris-HCl (pH 7.0) over 24 h using dialysis tubing with a molecular weight cutoff of 12–14 kDa. The dialyzed solution was concentrated, filtered using a 0.45  $\mu$ m membrane filter, and used as a source of crude enzyme for further experiments.

**Purification using fast protein liquid chromatography** All chromatographic purification steps were performed at 4°C using an ÄKTA prime plus system (GE Healthcare, Piscataway, NJ, USA) equipped with an ultraviolet (UV) detector. The crude protein was applied to a Hitrap DEAE-sepharose FF column (1.6  $\times$  2.5 cm) equilibrated with 50 mM Tris-HCl buffer (pH 9.0) at a flow rate of 5 mL min<sup>-1</sup>, and then the proteins bound to the column were eluted stepwise using 0.05, 0.10, 0.15, 0.20, and 1.0 M NaCl. Fractions with the highest  $\beta$ -glucosidase activity were collected, desalted, and concentrated by ultrafiltration using a membrane with a 10 kDa molecular weight cutoff. The pooled  $\beta$ -glucosidase fraction was loaded onto a Hitrap Q-sepharose XL (0.7  $\times$  2.5 cm) column equilibrated with 50 mM Tris-HCl buffer (pH 8.0) at a flow rate of 1.0 mL min<sup>-1</sup>. The column-bound proteins were eluted stepwise using 0.05, 0.10, 0.15, 0.20, and 1.0 M NaCl, and fractions with the highest  $\beta$ -glucosidase activity were collected, desalted, and concentrated by ultrafiltration. Then, the pooled  $\beta$ -glucosidase fraction was purified using a HiPrep 16/60 Sephacryl S-100 (1.6  $\times$  60 cm) column and 50 mM Tris-HCl buffer (pH 7.0) containing 0.15 M NaCl at a flow rate of 0.4 mL min<sup>-1</sup>. Fractions containing  $\beta$ -glucosidase activity were pooled, concentrated, and used for all biochemical and structural characterizations.

**Analysis of  $\beta$ -glucosidase activity**  $\beta$ -Glucosidase activity was determined using pNPG as the substrate, by monitoring the absorbance at 400 nm of the *p*-nitrophenol (pNP) liberated from pNPG. The reaction mixture (4 mL) containing 5 mM pNPG in Mcllvaine buffer (50 mM citrate/100 mM sodium phosphate buffer, pH 5.0) was incubated with the enzyme solution at 70°C. Aliquots (0.5 mL) of the reactant were collected at 10-min intervals for 30 min and mixed with 0.5 mL 400 mM Na<sub>2</sub>CO<sub>3</sub> to stop the reaction. One unit of enzyme activity was defined as the amount of enzyme required to release 1  $\mu$ mol pNP per minute. The protein concentration was determined according to the method of Bradford (17).

**Polyacrylamide gel electrophoresis** SDS-polyacrylamide gel electrophoresis (SDS-PAGE) was performed on a 12% resolving gel and a 5% stacking gel according to the method of Laemmli (18), in which 2-mercaptoethanol was used as a reducing agent. Samples were prepared by mixing purified enzyme with sample buffer containing 4% SDS, 20% (v/v) glycerol, 0.05% (w/v) bromophenol blue, and 10% (v/v) 2-mercaptoethanol and then boiled for 2 min at 100°C before loading onto the gel. All PAGE analyses were performed using the Hoefer SE 250 mini-gel system (GE Healthcare) at room temperature and a constant current of 20 mA. Migrated proteins were stained with Coomassie Brilliant Blue R-250. Native-PAGE was performed using the same method used for SDS-PAGE but without the use of SDS and 2-mercaptoethanol in the stacking buffer, resolving buffer, sample buffer, or boiling procedure.

To elucidate the interaction between two subunits of the purified enzyme, PAGE was conducted under three conditions. First, the sample was denatured using 4% SDS, reduced using 2-mercaptoethanol at 25°C, and subjected to SDS-PAGE. Second, the sample was denatured using 4% SDS in the absence of 2-mercaptoethanol and then subjected to SDS-PAGE. Third, the sample was subjected to native-PAGE in the absence of SDS and 2-mercaptoethanol.

**Zymography** Native-PAGE of  $\beta$ -glucosidase was performed using the method of Laemmli, except that the enzyme solutions were not heat-denatured, and SDS and reducing agent were left out before electrophoresis. After electrophoresis, the gel was equilibrated in Mcllvaine buffer (pH 4.0) for 15 min and then superposed on 1.0% agar containing 10 mM 4-MUG. The hydrolytic activity toward 4-MUG was visualized by UV light after incubation at 37°C for 24 h.

**Effects of temperature and pH on the enzyme** The effects of pH and temperature on the enzyme activity were determined by measurement of relative activity using pNPG as the substrate. The optimum pH for enzyme activity was determined by measuring the activity in Britton–Robinson buffer at 70°C over a pH range of 2.0–11.0, and the optimum temperature for enzyme activity was determined by measuring the activity in Mcllvaine buffer at pH 4.0 over a temperature range of 40–80°C. The pH stability of the enzyme was estimated by measuring the residual activity of each enzyme solution after incubation in Britton–Robinson buffer for 24 h at 4°C over a pH range of 2.0–12.0. The thermostability of the enzyme was estimated by measuring the residual activity of each enzyme solution after incubation in Mcllvaine buffer (pH 4.0) for 30 min over a temperature range of 30–90°C.

**Enzyme kinetics** The kinetic parameters ( $V_{max}$ ,  $K_m$ ,  $k_{cat}$ , and  $k_{cat}/K_m$ ) of purified  $\beta$ -glucosidase were determined from Hanes–Woolf linear transformation, which provides much higher accuracy for kinetic constant determination compared with the Michaelis–Menten equation. The enzyme reaction was initiated using 0.5 mg mL<sup>-1</sup>  $\beta$ -glucosidase at pH 4.0 and 70°C using pNPG as a substrate within the concentration range of 0.5–12 mM.

**Amino acid analysis** The amino acid composition of  $\beta$ -glucosidase was analyzed using a high-performance liquid chromatography instrument (Agilent 1200LC, Agilent Technologies, Inc., Santa Clara, CA, USA) equipped with a C18 column (5  $\mu$ m, 4.6  $\times$  150 mm), fluorescence detector (excitation wavelength of 340 nm, emission wavelength of 450 nm), and UV detector (338 nm).  $\beta$ -Glucosidase was hydrolyzed in 6 N HCl at 130°C for 24 h. Additionally, a calibration chromatogram was established for 21 known amino acids (aspartate, alanine, arginine, glutamate, glycine, serine, histidine, phenylalanine, proline, threonine, tyrosine, valine, isoleucine,  $\gamma$ -aminobutyric acid, leucine, lysine, asparagine, glutamine, norvaline, sarcosine, and hydroxyproline). Mobile phases A and B were 20 mM sodium phosphate monobasic buffer (pH 7.8) and water/methanol/acetone/nitrile (10:45:45 v/v/v), respectively, at a flow rate of 1.5 mL min<sup>-1</sup> for 30 min.

**Circular dichroism** Circular dichroism (CD) has become recognized as a powerful optical spectroscopic technique for examining protein structures in solution. In this study, measurements were performed on homogeneous  $\beta$ -glucosidase at a concentration of 0.1 mg mL<sup>-1</sup>. CD spectrometry (Chirascan-plus CD Spectrometer, Applied Photophysics, Ltd., Leatherhead, Surrey, UK) was performed in 10 mM sodium acetate (pH 4.0) in the far-UV region (190–260 nm) using a bandwidth of 1.0 nm and path length of 0.5 mm. To assess the effects of temperature on the secondary structure of  $\beta$ -glucosidase, CD was measured at different temperatures over the range of 30–85°C. The estimated percentages of the secondary structures detected from the CD spectra were calculated using CDNN software package (version 2.1).

## RESULTS AND DISCUSSION

**Purification of  $\beta$ -glucosidase from pumpkin seeds** The crude enzyme solution prepared by protein fractionation of the crude extract using the ammonium sulfate precipitation method was further purified by anion exchange and gel permeation chromatography according to the procedure summarized in Table 1. Finally, the highly purified enzyme of 15.1 mg was obtained from pumpkin seeds of 200 g. The overall yield of the purification was

**TABLE 1.** Summary of purification steps of  $\beta$ -glucosidase from pumpkin (*Cucurbita moschata*) seed.

Step	Total protein (mg)	Total activity (units)	Specific activity (units mg <sup>-1</sup> )	Yield (%)	Purification fold
Crude extract	2237.5	45.151	0.0202	100.00	1.00
10–80% (NH <sub>4</sub> ) <sub>2</sub> SO <sub>4</sub> precipitation	852.8	32.211	0.0378	71.34	1.87
DEAE-sepharose FF	129.6	11.473	0.0885	25.41	4.39
Q-sepharose XL	68.0	6.231	0.0916	13.80	4.54
Sephacryl S-100	15.1	2.503	0.1662	5.54	8.24
Hiresolution					

approximately 5.54%, with a purification fold of 8.24, and the purified  $\beta$ -glucosidase yielded  $16.62 \times 10^{-2}$  units  $\text{mg}^{-1}$  specific activity. Although the enzyme recovery yield seems to be lower than that of other  $\beta$ -glucosidases, it can be improved by changing the ionic strength of the medium, precipitating the enzyme with alcohols, and applying affinity chromatography. Fig. 1 shows the elution pattern of the enzyme during the four chromatography steps. To confirm the degree of purification, gel permeation chromatography was performed again, and a single peak representing the purified protein was detected (Fig. 1D). To determine the molecular mass of  $\beta$ -glucosidase, gel permeation chromatography using HiPrep 16/60 Sephacryl S-100 Hiresolution was performed once more, and a molecular mass of approximately 42.8 kDa was determined by reference to the calibration proteins (Fig. 2). The size of the enzyme was similar to those of *Galleria mellonella* (42 kDa), *Candida peltata* (43 kDa), and *Withania somnifera* (50 kDa) which exist as a monomer but smaller than those of *Malus domestica* (120 kDa), *Vanilla planifolia* (201 kDa), and *Secale cereal* (300 kDa) which exist as an oligomer (19–24). SDS-PAGE was performed to verify the purity and molecular mass of the enzyme. However, we detected two bands representing the  $\alpha$ -subunit and  $\beta$ -subunit, with molecular masses of 28.0 and 20.1 kDa, respectively, and this was not consistent with the previous result from gel permeation chromatography showing a single symmetrical peak (Supplementary Fig. S1). Therefore, the  $\beta$ -glucosidase appeared to be heterodimeric in nature, although the two proteins were co-eluted, and remained together in all of the chromatography columns tested. In addition, the lower molecular mass of  $\beta$ -glucosidase obtained from gel permeation chromatography compared with SDS-PAGE indicated that the heterodimeric protein is compact and spherical, rather than oval, such that the Stokes radius is minimized; on the other hand, calibration proteins form slightly elongated shapes (25).

**Optimum pH and temperature** The optimum pH and temperature of the purified  $\beta$ -glucosidase were estimated using pNPG

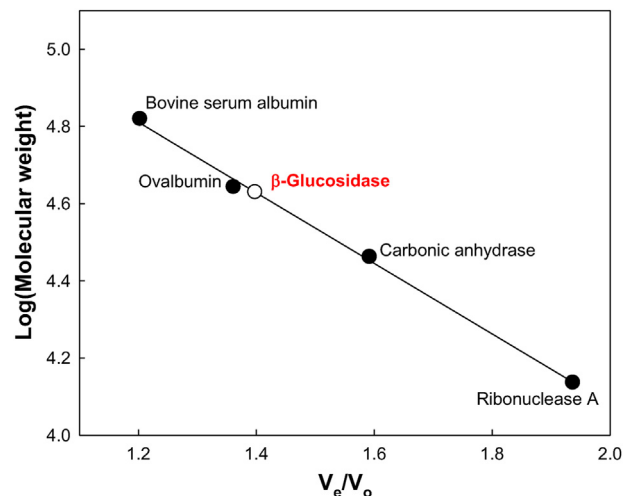


FIG. 2. Determination of molecular mass of  $\beta$ -glucosidase from pumpkin (*Cucurbita moschata*) seed.  $\beta$ -Glucosidase was loaded on HiPrep 16/60 Sephacryl S-100 HR with calibration proteins.  $V_e$  and  $V_o$  represent the elution volume and the void volume for each protein, respectively.

as a substrate. Fig. 3A shows the effect of pH on enzyme activity. The optimum pH for  $\beta$ -glucosidase activity was determined to be pH 4.0 and the activity was slightly reduced at pH 3.0.  $\beta$ -Glucosidase was inactivated at pH 2.0, and the activity decreased very rapidly at pH values higher than pH 5.0. It was unusual that the activity of  $\beta$ -glucosidase at pH 3.0 was not significantly different from that of the optimum pH. The reason why the enzyme is stable and active at pH 3.0 might be explained by ion-pair effect in active site of pepsin (26). It has been well known that glutamate is a key active site residue conserved in all  $\beta$ -glucosidases. The catalytic glutamate residues should not be

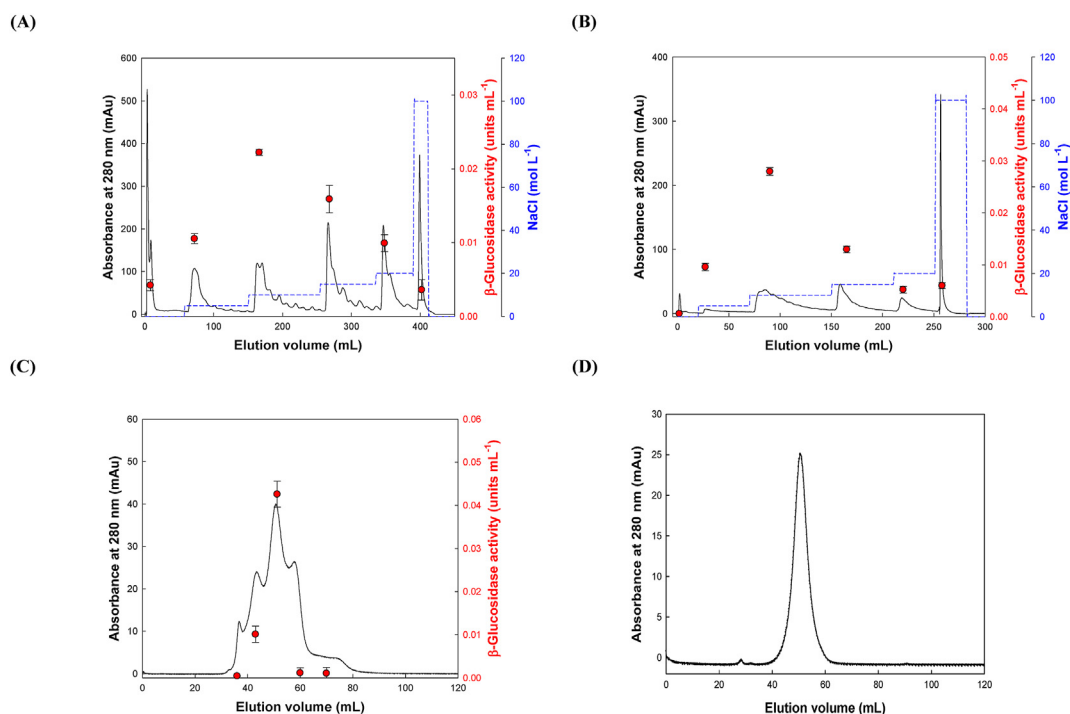


FIG. 1. Sequential chromatography for purification of  $\beta$ -glucosidase from pumpkin (*Cucurbita moschata*) seed. (A) Anion exchange chromatography with Hitrap DEAE FF. (B) Anion exchange chromatography with Hitrap Q XL. (C) The first gel permeation chromatography with HiPrep 16/60 Sephacryl S-100 HR. (D) The second gel permeation chromatography with HiPrep 16/60 Sephacryl S-100 HR. Symbols: solid line, absorbance at 280 nm; closed circles,  $\beta$ -glucosidase activity; dashed line, concentration of sodium chloride.

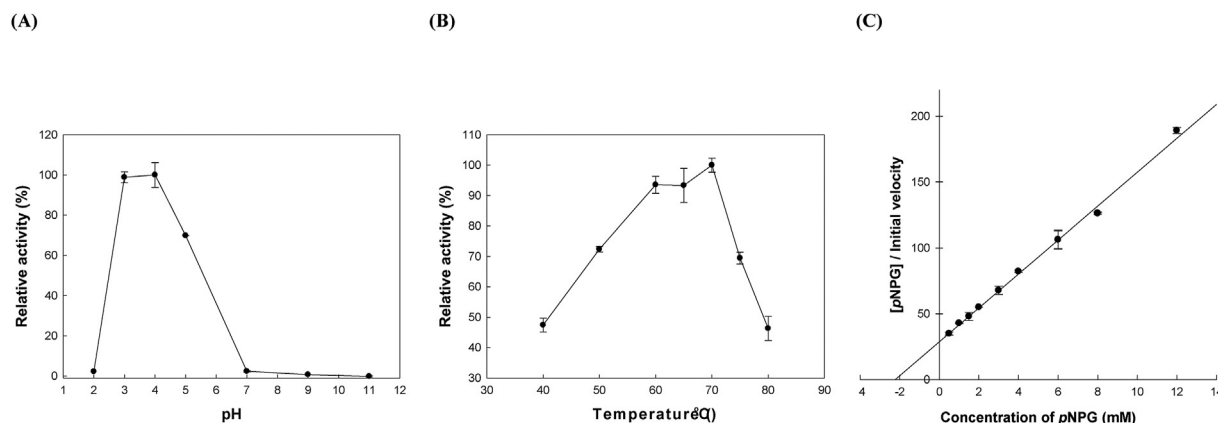


FIG. 3. Determination of optimum reaction conditions and kinetic parameters. Effects of (A) pH and (B) temperature on the catalytic activity of  $\beta$ -glucosidase from pumpkin (*Cucurbita moschata*) seed. (C) Hanes-Woolf plot for determination of the kinetic constants under the optimum conditions.

protonated in the range of low pH values for catalytic activity. Hence, it is likely that the carboxylate of glutamate residues interacts intimately through direct hydrogen-bonding with adjacent guanidinium group of arginine residues, resulting in neutralization of the two charges even below pH 3.0. The disposition of these groups might allow  $\beta$ -glucosidase to be stable and active in the strong acid media.

The acid-tolerant properties of this enzyme were comparable with the results reported for fungal  $\beta$ -glucosidases, e.g., *Agaricus bisporus* and *Aspergillus aculeatus*, but stronger than those of other microorganisms and plants (23,27–29). A comparison of acid-tolerant properties and kinetic parameters with other  $\beta$ -glucosidases is shown in Table 2. The narrow catalytic pH range can be explained by interaction modes at heterodimer interfaces. Several studies have shown that heterodimer interfaces composed of non-identical monomer subunits generally undergo hydrophilic interactions, whereas homodimer interfaces composed of identical monomer subunits undergo hydrophobic interactions (30). Thus, this catalytic pH range is not surprising because hydrophilic residues, which are dominant at heterodimer interfaces, where catalytic activity occurs, are easily affected by pH.

The effect of temperature on  $\beta$ -glucosidase activity was determined by evaluating enzyme activity at pH 4.0 using varying temperatures. A profile of the effect of temperature on enzyme activity is shown in Fig. 3B. Under the optimum pH, the purified enzyme showed 90% of its maximum enzyme activity at temperatures exceeding 60–70°C, and the optimum temperature was 70°C.

**Enzyme kinetics** The kinetic parameters of the purified enzyme ( $V_{\max}$ ,  $K_m$ ,  $k_{\text{cat}}$ , and  $k_{\text{cat}}/K_m$ ) were determined from a Hanes–Woolf plot (Fig. 3C) for pNPG under the optimum conditions (pH 4.0, 70°C). The  $V_{\max}$ ,  $K_m$ ,  $k_{\text{cat}}$ , and  $k_{\text{cat}}/K_m$  values were 0.078 units  $\text{mg}^{-1}$ , 2.22 mM, 13.29  $\text{min}^{-1}$ , and 2.81  $\text{s}^{-1} \text{mM}^{-1}$ , respectively. Enzyme kinetic studies indicate that the dissociation constant,  $K_m$ , is related to the association between subunits. Dimeric  $\beta$ -glucosidase of pumpkin seeds showed a five-fold lower  $K_m$  than that of monomeric  $\beta$ -glucosidase from the honey sac and ventriculus of honeybees (*Apis mellifera*), but the  $K_m$  of pumpkin seed  $\beta$ -glucosidase was similar to or slightly higher than those of hexameric  $\beta$ -glucosidases of rye (*S. cereal*) and wheat (*Triticum aestivum*) (31,32). These results are consistent with studies of the oligomeric structure of  $\beta$ -glucosidase (33). They revealed that larger multimers have higher affinity to substrates than do smaller multimers, and that the largest multimers hydrolyze the  $\beta$ -glycosidic linkage at a lower rate compared with the hexamer, although the functional implications of such a diverse multimerization still remain unclear.

**pH and temperature stability** To investigate the pH stability, the purified enzyme was incubated at various pH values. The pH-stability profile, shown in Fig. 4A, revealed that the enzyme is highly stable over a broad pH range. As shown in the profile, residual activities exceeding 80% were recovered between pH 2.0 and 10.0 after pre-incubation for 24 h at 4°C. The enzyme even

TABLE 2. Acid-tolerant properties of  $\beta$ -glucosidase from various sources.

Source	M.W. (kDa)	Opt. temp. (°C)	Opt. pH	pH stability	$K_m$ (mM)	$V_{\max}$ (units $\text{mg}^{-1}$ )	$k_{\text{cat}}$ ( $\text{s}^{-1}$ )	Ref.
<i>Cucurbita moschata</i>	48.1	70	4.0	2.0–10.0	2.22	0.078	0.222	This study
<i>Tolyposcladium cylindrosporium</i>	58.6	60	2.4	—	0.85	85.23	—	39
<i>Aspergillus aculeatus</i>	136	65	3.0	2.5–6.0	—	—	—	40
<i>Cellulomonas gilvus/Thermotoga maritima</i>	80	60	3.0, 5.0	3.0–5.0	0.012	—	5.62	41
<i>Ceriporiopsis subvermisporea</i>	110	60	3.5	—	3.29	0.113 $\times 10^{-3}$	—	42
<i>Candida molischiana</i>	380	55	3.5	—	—	—	—	43
<i>Paecilomyces Bainier</i> sp. 229	305	55	3.5	3.0–7.0	0.111	0.218	—	44
<i>Thermofilum pendens</i>	77.8	90	3.5	3.0–4.0	0.189	—	0.577	45
<i>Aspergillus pulverulentus</i> YM-80	118	60	4.0	3.0–7.0	—	—	—	46
<i>Evernia prunastri</i>	311	60	4.0	—	0.635	0.087 $\times 10^{-3}$	—	47
<i>Agaricus bisporus</i>	108	55	4.0	—	1.751	833	—	27
<i>Talaromyces emersonii</i>	90.59	71.5	4.02	—	0.13	512	2225.7	48
<i>Sulfolobus solfataricus</i>	313	70	4.0	—	4.15	—	9.15	49
<i>Thermoascus aurantiacus</i>	157	75	4.0	5.5–8.5	1.38	—	—	50
<i>Trichoderma reesei</i>	114	60	4.0	3.6–8.0	0.135	72.5	137.7	51

All data were obtained with pNPG as substrate.

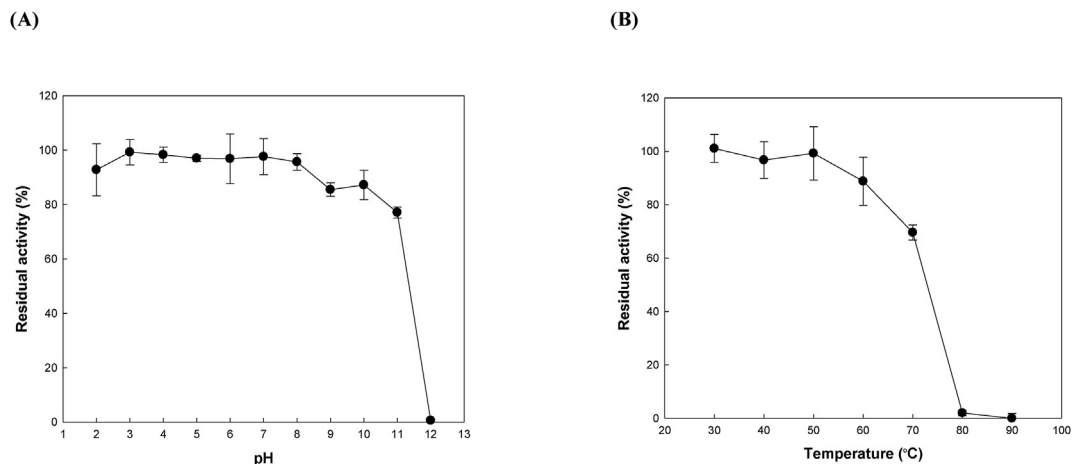


FIG. 4. Stable ranges of (A) pH and (B) temperature for the activity of  $\beta$ -glucosidase from pumpkin (*Cucurbita moschata*) seed.

retained approximately 93% of its original activity at pH 2.0. From pH 2.0 to 11.0, the positively or negatively charged structures of the enzyme were able to remain in a molten globule state, which allows them to be refolded as native structures. However, the structure became fully denatured at the extremely alkaline condition of pH 12.0.

The thermostability profile of the purified  $\beta$ -glucosidase (Fig. 4B) was determined by measuring the residual activity after incubation in McIlvaine buffer (pH 4.0) for 30 min at over a temperature range of 30–90°C. The enzyme was highly stable at temperatures below 50°C but was inactivated at temperatures greater than 70°C. The residual activity at 70°C, the optimum temperature, was approximately 70%, which implies that the enzyme is not stable and is thermally denatured at the optimum temperature.

**Effect of the interaction between the subunits on enzyme activity** Dissociation of inter- and intramolecular disulfide bonds was investigated to determine the detailed structure of  $\beta$ -glucosidase, which is stable over a broad pH range and exists as a heterodimer, as revealed by electrophoretic mobility assays under both reducing and denaturing conditions (Fig. 5). Under denaturing (presence of SDS) but nonreducing conditions (absence of 2-mercaptoethanol), the enzyme also migrated as a dimer. When the enzyme was reduced with 2-mercaptoethanol and then subjected to native-PAGE (in the absence of SDS), the single protein band was observed. Therefore, considering the above results comprehensively,  $\beta$ -glucosidase is not composed of disulfide-linked dimers; rather, the two subunits form a non-covalent bond, which is easily broken by SDS. These findings

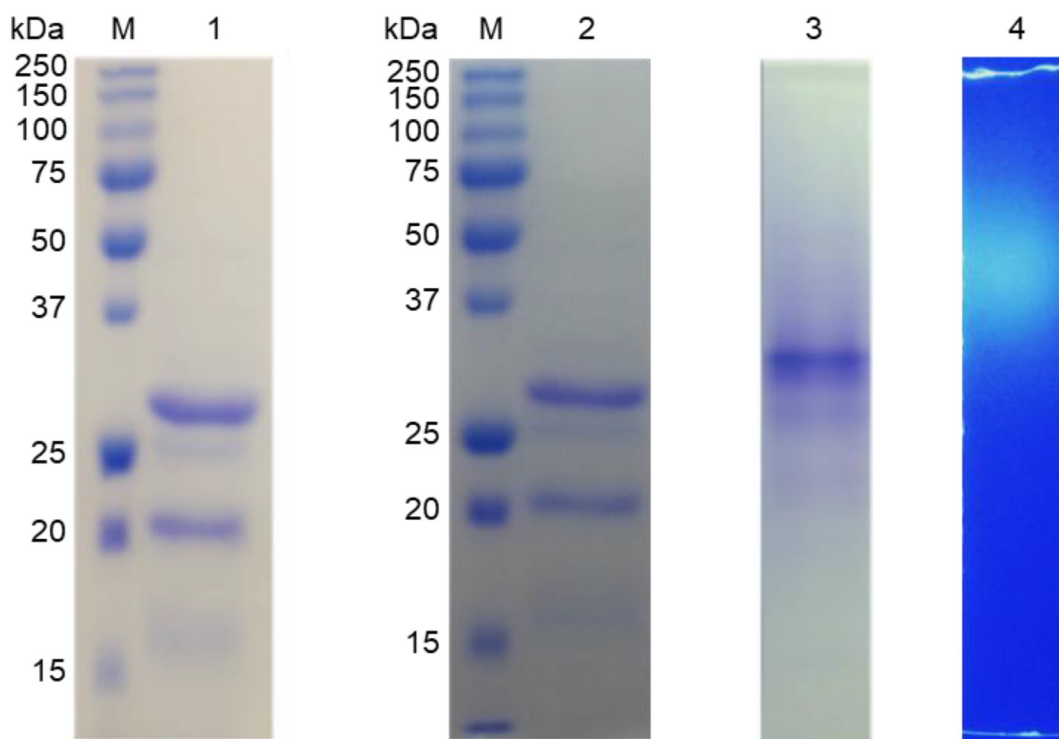


FIG. 5. Effect of the interaction between the subunits of  $\beta$ -glucosidase on catalytic activity. Lane M, molecular weight standard protein marker; lane 1, electrophoresis of  $\beta$ -glucosidase in the presence of SDS and 2-mercaptoethanol; lane 2, electrophoresis of  $\beta$ -glucosidase in the presence of SDS and absence of 2-mercaptoethanol; lane 3, electrophoresis of  $\beta$ -glucosidase in the absence of SDS and 2-mercaptoethanol; lane 4, catalytic activity of the migrated protein in lane 3 toward the fluorescent compound (4-MUG).

show distinctive difference from other  $\beta$ -glucosidases of maize (*Zea mays*), rice (*Oryza sativa*), rye (*S. cereal*), and wheat (*T. aestivum*), which are composed of one disulfide bond (32,34).

Furthermore, to investigate whether each subunit of  $\beta$ -glucosidase exhibits enzyme activity independently, zymography was conducted under the native condition after native-PAGE without staining. The zymography result showed that only the native enzyme possesses distinct activity toward the fluorescent compound (4-MUG) (Fig. 5, lane 4). Therefore, the enzyme exhibits activity only in the native form, in which the subunits are associated. This result is consistent with those of multimeric  $\beta$ -glucosidases from wheat and rye, which lose activity when separated into monomers or smaller oligomers (32). Thus, it appears that the active site region is located at the interface between the subunits, and that dimerization is essential for activity.

**Analysis of amino acid composition and secondary structure** To investigate the secondary structure of  $\beta$ -glucosidase, the number of amino acid residues was analyzed, as a prerequisite. As shown in Table 3, only 15 types of amino acids were detected because tryptophan, asparagine, methionine, and several other amino acids are destroyed by the acid treatment procedure and are not detected due to their low levels. Glycine was the most abundant essential amino acid in the enzyme, and cysteine was not detected. The high glycine content indicates that this enzyme possesses a highly flexible domain that acts as velcro for dimeric interactions and might be located at the plasma membrane-cell wall interface (35,36). The absence of cysteine supports the PAGE results indicating that the enzyme does not consist of disulfide bonds at sites of intra- or intermolecular interactions, which play an important role in enhancing protein stability (37).

Far-UV CD spectra reflecting the secondary structure of  $\beta$ -glucosidase were recorded between 190 and 260 nm. Negative bands at 208 and 222 nm and a positive band at 193 nm represent an  $\alpha$ -helix structure, a negative band at 218 nm and positive band at 195 nm represent a  $\beta$ -sheet structure, and negative bands at 189 and 198 nm and positive bands at 210 and 212 nm represent disordered structures such as  $\beta$ -turn and random coil structures (Fig. S2). Under the stable condition, the secondary structures of  $\beta$ -glucosidase consist of 26.10%  $\alpha$ -helices, 20.17% antiparallel  $\beta$ -sheets, 8.22% parallel  $\beta$ -sheets, 18.16%  $\beta$ -turns, and 27.34% random coil structures. To investigate the effect of temperature on secondary structure, the thermal profile was observed at different temperatures in the range of 30–85°C. The structural elements (%) of  $\beta$ -glucosidase at different temperatures and pH are shown in Table 4. With a temperature increase, the  $\alpha$ -helix content became smaller, but the antiparallel  $\beta$ -sheet content became larger, until reaching 85°C. The structure of the enzyme was affected only slightly by temperature changes, but structural changes were greater at high

**TABLE 4.** Proportions (%) of the structural elements in  $\beta$ -glucosidase at different temperatures and pH.

Temperature (°C)	pH	$\alpha$ -helix (%)	Antiparallel $\beta$ -sheet (%)	Parallel $\beta$ -sheet (%)	$\beta$ -turn (%)	Random coil (%)
30	2.0	23.06	41.39	4.99	18.85	11.70
30	4.0	26.10	20.17	8.22	18.16	27.34
30	8.0	33.06	11.73	8.16	17.96	29.08
40	4.0	25.09	21.13	8.21	18.11	27.45
50	4.0	23.55	23.55	8.13	18.01	26.78
60	4.0	21.70	27.68	7.86	17.95	24.82
70	4.0	21.30	28.31	7.81	17.92	24.67
80	4.0	21.46	28.41	7.75	17.90	24.49
85	4.0	19.11	26.91	8.57	17.14	28.28

temperatures approaching 85°C. This phenomenon can be explained by the mechanism of  $\alpha$ -helix to  $\beta$ -sheet transformation (38). When supplied with thermal energy, the  $\alpha$ -helical structure unfolds and then converts into an antiparallel  $\beta$ -sheet structure via a random coil state. Moreover, this transition might be triggered by initial helix–helix interactions. The dramatic change in secondary structure induced by pH was in contrast to the effect induced by temperature. As can be inferred from the pH stability test, this conformational change is caused by changes in amino acid residues, resulting in heterodimer dissociation; nevertheless, the change is reversible and thus the activity of the enzyme can be recovered under optimum pH conditions.

In conclusion,  $\beta$ -glucosidase exhibiting  $V_{max}$ ,  $K_m$ , and  $k_{cat}$  values of 0.078 units  $mg^{-1}$  protein, 2.22 mM, and 13.29  $min^{-1}$ , respectively, toward the substrate pNPG was successfully purified from pumpkin (*C. moschata*) seeds. The enzyme, involving hydrophilic interactions between the  $\alpha$ -subunit (28.0 kDa) and  $\beta$ -subunit (20.1 kDa), showed a reversible conformational change across a broad pH range of 2.0–11.0 due to its simple tertiary structure free from disulfide bonds. In particular, the assembly mode of  $\beta$ -glucosidase is very unique in that it dimerizes heterogeneously by secondary interactions only. The high glycine and hydrophobic amino acid contents suggest that the enzyme possesses a flexible velcro region involved in interactions between proteins and with cell membranes and walls, implying that this enzyme may be related to cell wall remodeling, lignification, or chemical defense. Furthermore, the acid-tolerant characteristics of  $\beta$ -glucosidase imply that this enzyme would be active even in the human stomach at pH 3.5–5.0 and would be useful for the production of acidic beverages, such as orange and grape juices, and fermented products containing isoflavone-rich ingredients.

Supplementary data to this article can be found online at <https://doi.org/10.1016/j.jbiosc.2021.04.004>.

## ACKNOWLEDGMENTS

This work was supported by Cooperative Research Program for Agriculture Science & Technology Development (Project No. PJ01488801) provided by Rural Development Administration, Republic of Korea.

## References

- Liu, Y.-P., Guo, J.-M., Yan, G., Zhang, M.-M., Zhang, W.-H., Qiang, L., and Fu, Y.-H.: Anti-inflammatory and antiproliferative prenylated isoflavone derivatives from the fruits of *Ficus carica*. *J. Agric. Food Chem.*, **67**, 4817–4823 (2019).
- Mansoor, T. A., Ramalho, R. M., Luo, X., Ramalho, C., Rodrigues, C. M., and Ferreira, M. J. U.: Isoflavones as apoptosis inducers in human hepatoma HuH-7 cells. *Phytother. Res.*, **25**, 1819–1824 (2011).
- Gacche, R. N., Shegokar, H. D., Gond, D. S., Yang, Z., and Jadhav, A. D.: Evaluation of selected flavonoids as antiangiogenic, anticancer, and radical scavenging agents: an experimental and in silico analysis. *Cell Biochem. Biophys.*, **61**, 651–663 (2011).

**TABLE 3.** Amino acid composition of  $\beta$ -glucosidase from pumpkin (*Cucurbita moschata*) seed.

Amino acid	Mol.%	Number of residues <sup>a</sup>	Amino acid	Mol.%	Number of residues <sup>a</sup>
Aspartate (Asp)	10.4	38	Valine (Val)	6.2	23
Glutamate (Glu)	8.4	30	Proline (Pro)	6.0	22
Serine (Ser)	7.5	27	Phenylalanine (Phe)	3.1	11
Histidine (His)	2.8	10	Isoleucine (Ile)	4.4	16
Glycine (Gly)	18.4	67	Leucine (Leu)	7.8	28
Threonine (Thr)	5.4	20	Lysine (Lys)	5.4	20
Arginine (Arg)	2.8	10	Methionine (Met)	N.D.	N.D.
Alanine (Ala)	10.7	39	Cysteine (Cys)	N.D.	N.D.
Tyrosine (Tyr)	0.7	2	Tryptophan (Trp)	N.D.	N.D.

<sup>a</sup> The number of residues was calculated on the basis of a molecular mass of 42.8 kDa.

4. **Neves, M. V. M.d., Silva, T. M. S.d., Lima, E.d. O., Cunha, E. V. L.d., and Oliveira, E.d. J.:** Isoflavone formononetin from red propolis acts as a fungicide against *Candida* sp., *Braz. J. Microbiol.*, **47**, 159–166 (2016).
5. **Zheng, X., Lee, S.-K., and Chun, O. K.:** Soy isoflavones and osteoporotic bone loss: a review with an emphasis on modulation of bone remodeling, *J. Med. Food*, **19**, 1–14 (2016).
6. **Vitale, D. C., Piazza, C., Melilli, B., Drago, F., and Salomone, S.:** Isoflavones: estrogenic activity, biological effect and bioavailability, *Eur. J. Drug Metab. Pharmacokinet.*, **38**, 15–25 (2013).
7. **Ketudat, C. J. and Esen, A.:**  $\beta$ -Glucosidases, *Cell. Mol. Life Sci.*, **67**, 3389–3405 (2010).
8. **Swangkeaw, J., Vichitphan, S., Butzke, C. E., and Vichitphan, K.:** Characterization of  $\beta$ -glucosidases from *Hanseniaspora* sp. and *Pichia anomala* with potentially aroma-enhancing capabilities in juice and wine, *World J. Microbiol. Biotechnol.*, **27**, 423–430 (2011).
9. **Singh, G., Verma, A., and Kumar, V.:** Catalytic properties, functional attributes, and industrial applications of  $\beta$ -glucosidases, *3 Biotech*, **6**, 3 (2016).
10. **Fujita, A., Alencar, S., and Park, Y.:** Conversion of isoflavone glucosides to aglycones by partially purified  $\beta$ -glucosidases from microbial and vegetable sources, *Appl. Biochem. Biotechnol.*, **176**, 1659–1672 (2015).
11. **Medjakovic, S., Hobiger, S., Ardjomand-Woelkart, K., Bucar, F., and Jungbauer, A.:** Pumpkin seed extract: cell growth inhibition of hyperplastic and cancer cells, independent of steroid hormone receptors, *Fitoterapia*, **110**, 150–156 (2016).
12. **Patel, S.:** Pumpkin (*Cucurbita* sp.) seeds as nutraceutical: a review on status quo and scopes, *Med. J. Nutr. Metab.*, **6**, 183–189 (2013).
13. **El-Mosallamy, A. E., Sleem, A. A., Abdel-Salam, O. M., Shaffie, N., and Kenawy, S. A.:** Antihypertensive and cardioprotective effects of pumpkin seed oil, *J. Med. Food*, **15**, 180–189 (2012).
14. **Pujilestari, S., Sandrasari, D. A., and Marida, R.:** Chemical characteristics of pumpkin seed tempeh from soybean and pumpkin seeds, *ComTech*, **8**, 115–119 (2017).
15. **Shin, S. Y., Joung, K. Y., and Kim, Y.-S.:** Quality and texture characteristics of pumpkin seed tofu made with soybean (*Glycine max* L. Merrill) and pumpkin (*Cucurbita moschata* Duch.) seed, *J. Korean Soc. Food Sci. Nutr.*, **31**, 62–69 (2018).
16. **Marañón, J. A., Lozano, C., Martínez-Campesino, L., de Los Santos, L., Bank, G., and Caballero-Garrido, E.:** Clinical study: effect of supplementation with high genistein soybean isoflavones and pumpkin standardized extract on urinary incontinence in western perimenopausal women, *J. Gynecol. Women's Health*, **4**, 555627 (2017).
17. **Bradford, M. M.:** A rapid and sensitive method for the quantitation of microgram quantities of protein utilizing the principle of protein-dye binding, *Anal. Biochem.*, **72**, 248–254 (1976).
18. **Laemmli, U. K.:** Cleavage of structural proteins during the assembly of the head of bacteriophage T4, *Nature*, **227**, 680–685 (1970).
19. **Kara, H. E., Turan, Y., Er, A., Acar, M., Tümay, S., and Sinan, S.:** Purification and characterization of  $\beta$ -glucosidase from greater wax moth *Galleria mellonella* L. (Lepidoptera: Pyralidae), *Arch. Insect Biochem. Physiol.*, **86**, 209–219 (2014).
20. **Saha, B. C. and Bothast, R. J.:** Production, purification, and characterization of a highly glucose-tolerant novel beta-glucosidase from *Candida peltata*, *Appl. Environ. Microbiol.*, **62**, 3165–3170 (1996).
21. **Mishra, S. K., Sangwan, N. S., and Sangwan, R. S.:** Comparative physico-kinetic properties of a homogenous purified  $\beta$ -glucosidase from *Withania somnifera* leaf, *Acta Physiol. Plant.*, **35**, 1439–1451 (2013).
22. **Yu, H.-L., Xu, J.-H., Lu, W.-Y., and Lin, G.-Q.:** Identification, purification and characterization of  $\beta$ -glucosidase from apple seed as a novel catalyst for synthesis of *O*-glucosides, *Enzyme Microb. Technol.*, **40**, 354–361 (2007).
23. **Odoux, E., Chauwin, A., and Brillouet, J.-M.:** Purification and characterization of vanilla bean (*Vanilla planifolia* Andrews)  $\beta$ -D-glucosidase, *J. Agric. Food Chem.*, **51**, 3168–3173 (2003).
24. **Sue, M., Ishihara, A., and Iwamura, H.:** Purification and characterization of a  $\beta$ -glucosidase from rye (*Secale cereale* L.) seedlings, *Plant Sci.*, **155**, 67–74 (2000).
25. **Irvine, G. B.:** Determination of molecular size by size-exclusion chromatography (gel filtration), *Curr. Protoc. Cell Biol.*, **6**, 5.5.1–5.5.16 (2000).
26. **Sielecki, A. R., Fedorov, A. A., Boodhoo, A., Andreeva, N. S., and James, M. N.:** Molecular and crystal structures of monoclinic porcine pepsin refined at 1.8 Å resolution, *J. Mol. Biol.*, **214**, 143–170 (1990).
27. **Asić, A., Bešić, L., Muhović, I., Dogan, S., and Turan, Y.:** Purification and characterization of  $\beta$ -glucosidase from *Agaricus bisporus* (white button mushroom), *Protein J.*, **34**, 453–461 (2015).
28. **Liew, K. J., Lim, L., Woo, H. Y., Chan, K.-G., Shamsir, M. S., and Goh, K. M.:** Purification and characterization of a novel GH1 beta-glucosidase from *Jeotgilibacillus malaysiensis*, *Int. J. Biol. Macromol.*, **115**, 1094–1102 (2018).
29. **Cuevas, L., Niemeyer, H. M., and Jonsson, L. M.:** Partial purification and characterization of a hydroxamic acid glucoside  $\beta$ -D-glucosidase from maize, *Phytochemistry*, **31**, 2609–2612 (1992).
30. **Zhanhua, C. and Gan, J. G.-K.:** Protein subunit interfaces: heterodimers versus homodimers, *Bioinformatics*, **1**, 28–39 (2005).
31. **Pontoh, J. and Low, N.:** Purification and characterization of  $\beta$ -glucosidase from honey bees (*Apis mellifera*), *Insect Biochem. Mol. Biol.*, **32**, 679–690 (2002).
32. **Sue, M., Yamazaki, K., Yajima, S., Nomura, T., Matsukawa, T., Iwamura, H., and Miyamoto, T.:** Molecular and structural characterization of hexameric  $\beta$ -D-glucosidases in wheat and rye, *Plant Physiol.*, **141**, 1237–1247 (2006).
33. **Kim, S.-Y., Kim, Y.-W., Hegerl, R., Cyrklaff, M., and Kim, I.-S.:** Novel type of enzyme multimerization enhances substrate affinity of oat  $\beta$ -glucosidase, *J. Struct. Biol.*, **150**, 1–10 (2005).
34. **Zouhar, J., Védová, J., Marek, J., Damborský, J., Su, X.-D., and Brzobohatý, B.:** Insights into the functional architecture of the catalytic center of a maize  $\beta$ -glucosidase Zm-p60.1, *Plant Physiol.*, **127**, 973–985 (2001).
35. **Chichili, Reddy, Priyanka, V., Kumar, V., and Sivaraman, J.:** Linkers in the structural biology of protein-protein interactions, *Protein Sci.*, **22**, 153–167 (2013).
36. **Sachetto-Martins, G., Franco, L. O., and de Oliveira, D. E.:** Plant glycine-rich proteins: a family or just proteins with a common motif? *Biochim. Biophys. Acta Gene Struct. Expr.*, **1492**, 1–14 (2000).
37. **Liu, T., Wang, Y., Luo, X., Li, J., Reed, S. A., Xiao, H., Young, T. S., and Schultz, P. G.:** Enhancing protein stability with extended disulfide bonds, *Proc. Natl. Acad. Sci.*, **113**, 5910–5915 (2016).
38. **Qi, R., Luo, Y., Ma, B., Nussinov, R., and Wei, G.:** Conformational distribution and  $\alpha$ -helix to  $\beta$ -sheet transition of human amylin fragment dimer, *Biomacromolecules*, **15**, 122–131 (2014).
39. **Yi-bo, Z., Li-jia, Y., Zhao-jie, C., Lu, F., Jia-hui, L., Qing-fan, M., Huan, H., Xiaoxiao, Y., Feng, L., and Li-rong, T.:** Purification and characterization of beta-glucosidase from a newly isolated strain *Tolyopocladium cylindrosporum* Syzx4, *Chem. Res. Chin. Univ.*, **27**, 557–561 (2011).
40. **Murao, S., Sakamoto, R., and Arai, M.:** Cellulases of *Aspergillus aculeatus*, *Methods Enzymol.*, **160**, 274–299 (1988).
41. **Kim, J. D., Seo, H. J., and Hayashi, K.:** Construction and characterization of novel chimeric  $\beta$ -glucosidases with *Cellvibrio gilvus* (CG) and *Thermotoga maritima* (TM) by overlapping PCR, *Biotechnol. Bioprocess Eng.*, **14**, 266 (2009).
42. **Magalhaes, P., Ferraz, A., and Milagres, A.:** Enzymatic properties of two  $\beta$ -glucosidases from *Ceriporiopsis subvermisporea* produced in biopurification conditions, *J. Appl. Microbiol.*, **101**, 480–486 (2006).
43. **Janbon, G., Derancourt, J., Chemardin, P., Arnaud, A., and Galzy, P.:** A very stable  $\beta$ -glucosidase from a *Candida molischiana* mutant strain: enzymatic properties, sequencing, and homology with other yeast  $\beta$ -glucosidases, *Biosci. Biotechnol. Biochem.*, **59**, 1320–1322 (1995).
44. **Yan, Q., Zhou, W., Li, X., Feng, M., and Zhou, P.:** Purification method improvement and characterization of a novel ginsenoside-hydrolyzing  $\beta$ -glucosidase from *Paecilomyces Bainier* sp. 229, *Biosci. Biotechnol. Biochem.*, **72**, 352–359 (2008).
45. **Li, D., Li, X., Dang, W., Tran, P. L., Park, S.-H., Oh, B.-C., Hong, W.-S., Lee, J.-S., and Park, K.-H.:** Characterization and application of an acidophilic and thermostable  $\beta$ -glucosidase from *Thermofilum pendens*, *J. Biosci. Bioeng.*, **115**, 490–496 (2013).
46. **Mase, T., Mori, S., and Yokoe, M.:** Purification, characterization, and a potential application of beta-glucosidase from *Aspergillus pulverulentus* YM-80, *J. Appl. Glycosci.*, **51**, 211–216 (2004).
47. **Yagüe, E. and Estévez, M. P.:** Purification and characterization of a  $\beta$ -glucosidase from *Evernia prunastri*, *Eur. J. Biochem.*, **175**, 627–632 (1988).
48. **Murray, P., Aro, N., Collins, C., Grassick, A., Penttilä, M., Saloheimo, M., and Tuohy, M.:** Expression in *Trichoderma reesei* and characterisation of a thermostable family 3  $\beta$ -glucosidase from the moderately thermophilic fungus *Talaromyces emersonii*, *Protein Expr. Purif.*, **38**, 248–257 (2004).
49. **Ferrara, M. C., Cobucci-Ponzano, B., Carpentieri, A., Henrissat, B., Rossi, M., Amoresano, A., and Moracci, M.:** The identification and molecular characterization of the first archaeal bifunctional exo- $\beta$ -glucosidase/*N*-acetyl- $\beta$ -glucosaminidase demonstrate that family GH116 is made of three functionally distinct subfamilies, *Biochim. Biophys. Acta Gen. Subj.*, **1840**, 367–377 (2014).
50. **de Palma-Fernandez, E., Gomes, E., and Da Silva, R.:** Purification and characterization of two  $\beta$ -glucosidases from the thermophilic fungus *Thermoascus aurantiacus*, *Folia Microbiol. (Praha)*, **47**, 685–690 (2002).
51. **Chen, H., Hayn, M., and Esterbauer, H.:** Purification and characterization of two extracellular  $\beta$ -glucosidases from *Trichoderma reesei*, *Biochim. Biophys. Acta Protein Struct. Mol. Enzymol.*, **1121**, 54–60 (1992).